Eur. Phys. J. B **13**, 571–578 (2000)

**THE EUROPEAN PHYSICAL JOURNAL B**

EDP Sciences


# Experimental study of the porosity of loose stacks of stiff cylindrical fibres: Influence of the aspect ratio of fibres

M. Novellani[a], R. Santini, and L. Tadrist

Institut Universitaire des Systèmes Thermiques Industriels[b], Université de Provence, Technopôle de Château Gombert, 5 rue Enrico Fermi, 13453 Marseille Cedex 13, France

Received 12 April 1999 and Received in final form 4 August 1999

**Abstract.** The aim of this work is to study the porosity of three-dimensional and two-dimensional packing of stiff cylindrical fibres according to their aspect ratio. First, we have carried out an experimental study of the porosity for 3D and 2D packing. In this last case, the elementary representative surfaces have been determined. Then, an attempt of interpretation of the porosity variations for 2D stacks has been realized on the basis of the excluded volume theory and a variation law has been proposed. To conclude, we have studied the relevance of a simplified packing model based on a single geometry of the defects.

**PACS.** 45.70.-n Granular systems – 46.65.+g Random phenomena and media – 61.43.Gt Powders, porous materials

## 1 Introduction

Porous media present many different characteristics of structure (shape of the skeleton and of the pores of the solid matrix). There is also a great diversity in the material which compose them. We find them in our natural environment (beds of sand, of gravel, wood, foams, chalky soil, ...) as well as in manufactured goods (building materials, paper, insulators, catalysts, ...). Moreover a large number of industrial products such as glass wool, filters, reticulate ceramics, new composite materials are composed of fibres.

The present study concerns the characterisation of stacks of rigid fibres. Because of the complexity of these systems, the experimental approach is a good tool to study their structural characteristics (porosity, permeability, arrangement, etc.).

Many works concerning ordered and random stacks of spheres having one or several radii have been carried out since the thirties and literature is full of results in this field. Yet, the first experimental results concerning the packing of fibres appeared in the seventies.

Milewski [1–3] studied mixtures of fibres and glass beads to reduce the amount of resin used in making reinforced plastics. He made measurements on stacks of wooden fibres having a diameter of 2.1 mm and an aspect ratio $r = L/d$ (fraction length over the diameter of the fibre) between 4 and 72. He determined a law of variation for the density of the stack as a function of the aspect ratio of the fibre. He obtained the same law of variation for fibreglass having a diameter equal to 13 $\mu$m and has extended his study to the combinations of fibres with different aspect ratios.

Nardin [4] studied stacks of particles of different natures (glass, steel, PMMA ...) and of various shapes (spheres, discs, fibres, revolution ellipsoids). He distinguished two major types of stacks:

- loose, obtained by settling in a viscous fluid;
- close, obtained by compression of the stack (with small vibrations).

Rahli [5,6] studied loose and close packing of Nylon or metal (copper, bronze) fibres. He, moreover, proposed a model based on the excluded volume determined by Onsager [7]. With this model, the variations of porosity can be described according to the aspect ratio.

Parkhouse and Kelly [8] studied the packing of spaghetti having a diameter of 1.8 mm and an aspect ratio between 6 and 140. Thanks to a semi-empirical model, these authors proposed an analytic expression of the law of porosity as a function of the aspect ratio. They also defined an upper limit to the solid volume fraction for each aspect ratio.

The major results acquired on the packing of rigid fibres are the following:

- the existence of a single variation curve of the porosity according to the aspect ratio for loose packing, whatever the nature or the size of the fibres;
- the existence of two models of variation of the porosity.

All these works concern three-dimensional stacks of rigid fibres.

[a] e-mail: novel@iusti.univ-mrs.fr
[b] UMR 6595 du CNRS

The subject of the present work is the study of the loose packing of cylindrical fibres made of plastic, having a diameter equal to 5 mm and an aspect ratio between 1.2 and 50.5, for three-dimensional and two-dimensional stacks, with particular attention to the 2D structures. In this last case, the width of the packing cell is equal to the diameter of a fibre. These two-dimensional structures present many advantages in experiments as well as in theory. In this configuration, it is possible to study the structure of the stack. In this work, the variation laws of the porosity according to the aspect ratio are determined experimentally for 2D and 3D stacks. For 2D stacks, a variation law of the porosity is proposed.

## 2 Materials and methods

### 2.1 Fibres and packing cells

The fibres used are cylinders in white delrin (plastic) having a diameter of 5 mm. Their aspect ratios are contained between 1.2 and 50.5.

For 2D stacks, 3 different-sized glass cells, adapted to the lengths of the fibres, are used. The dimensions of the cells (Width $W$ and Height $H$) and the aspect ratios of the fibres which can be studied are the following:

| | cell | | |
|---|---|---|---|
| | 1 | 2 | 3 |
| $W$ (cm) | 18.6 | 38 | 100 |
| $H$ (cm) | 50 | 50 | 100 |
| $r$ | 1.2 | 3.0 | 12.1 |
| | 1.5 | 5.0 | 20.2 |
| | 3.0 | 7.1 | 30.3 |
| | | 10.1 | 50.5 |
| | | 12.1 | |

To obtain stacks in 2D cells, two methods are possible. The first consists in using a funnel in the shape of a triangular prism whose rectangular outlet is equal to the aperture of the cell. In this case, fibres are simply poured into the funnel and then drop into the cell. The packing is made without any compression, so the stacks obtained are loose. The second method consists in introducing the fibres individually by hand, with a position and an orientation as random as possible. The second method has not been used in this study because it is too time-consuming for the small aspect ratios. Two examples of 2D stacks are presented in Figure 1 (Photos 1 and 2).

### 2.2 Analysis tools

#### 2.2.1 Determining the porosity of 2D and 3D stacks by weighing

The method of measuring the porosity $\varepsilon_{\mathrm{p}}$ by weighing is very simple but it enables only the mean porosity of all the stack to be ascertained. In particular, it integrates the possible local variation of porosity due to the effects of the sides of the cell. Once the density $\rho$ of the delrin and the total volume $V_{\mathrm{tot}}$ occupied by a mass $m$ of fibres (equivalent to a volume of fibres $V_{\mathrm{f}}$) are known, the mean porosity $\varepsilon_{\mathrm{p}}$ of the stack is:

$$\varepsilon_{\mathrm{p}} = 1 - \frac{V_{\mathrm{f}}}{V_{\mathrm{tot}}} = 1 - \frac{m}{\rho}\frac{1}{V_{\mathrm{tot}}} \cdot \qquad (1)$$

The uncertainty of the measurement of the mean stack height leads to an error $\Delta V_{\mathrm{tot}}$ over the total volume $V_{\mathrm{tot}}$. So, at first approximation, the error on porosity is:

$$\Delta\varepsilon_{\mathrm{p}} \approx \frac{V_{\mathrm{f}}\,\Delta V_{\mathrm{tot}}}{V_{\mathrm{tot}}^2} \cdot \qquad (2)$$

The 2D porosities have been obtained by averaging the values found for 3 different stacks for each aspect ratio. The deviations from the mean value are smaller than 0.5%.

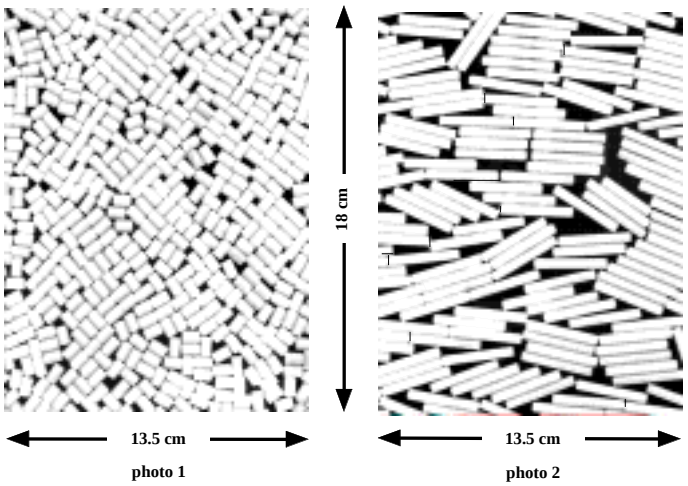


**Fig. 1.** Photo 1: Part of a stack of fibres having an aspect ratio $r = 1.5$. Photo 2: Part of a stack of fibres having an aspect ratio $r = 7.1$.

#### 2.2.2 Determining the porosity and the local properties of 2D stacks by image processing

Image processing enables the local porosity of the system on a defined surface to be studied and then the problems due to the boundaries of the stack to be minimised. The experimental set-up used is shown in Figure 2. The images are processed and the two-dimensional porosity of the stack is given by the fraction number of black pixels over the total number of pixels of the complete image. To obtain a porosity in a volume, it is necessary to apply a conversion factor to the result because fibres are cylinders and not parallelepipeds.

We have assessed the porosities of the stacks in central rectangular windows of increasing sizes. As can be seen in

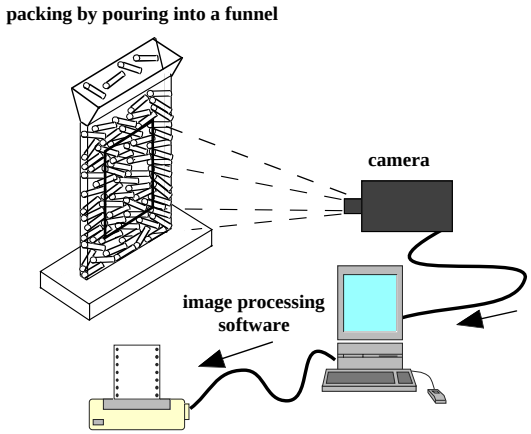


**Fig. 2.** Experimental set-up used to study 2D packing by image processing.

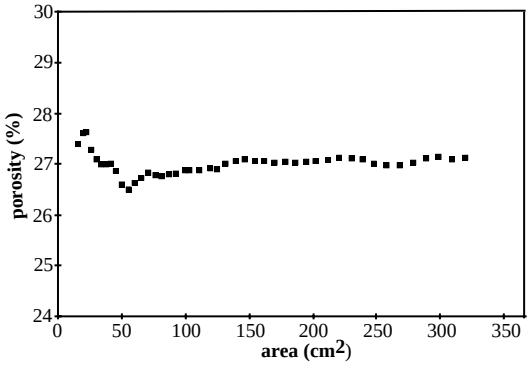


**Fig. 3.** Porosity for 2D packing *versus* the area of the observation window - $r = 1.5$.

Figures 3 and 4, the curves which represent the variations of the porosity according to the size of the window have two distinct parts:

- a first part where the porosity varies noticeably;
- a second part where the porosity fluctuates around a mean value; the range of these fluctuations decreases when the area of the observation window increases.

So, we define the Elementary Representative Surface (ERS) as the smallest area for which the porosity becomes almost constant. In practice, the ERS is taken as the area after which the maximum deviation between two extreme values of porosity is less than one percent of the average of these values. Then, the mean porosity found by image analysis is defined as the average of the measured porosities for areas larger than the ERS.

Thus, the ERS determined for aspect ratios equal to 1.5 - 3 (cell 1) - 5.0 - 7.1 and 10.1 (cell 2) are given in Table 1. In Figure 5, we have drawn the variations of the dimensionless ERS ($\mathrm{ERS^d}$), defined as the fraction ERS over the apparent area of a fibre $S_\mathrm{f}$ ($S_\mathrm{f} = L \times d$), *versus* the aspect ratio. The ERS is noticeably proportional to $r$. Therefore the $\mathrm{ERS^d}$ is almost constant. For the studied

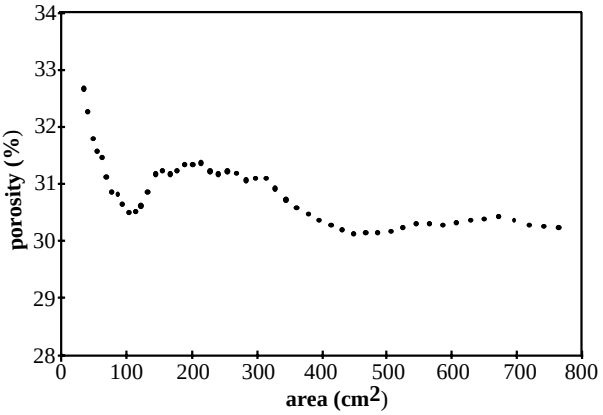


**Fig. 4.** Porosity for 2D packing *versus* the area of the observation window - $r = 5.0$.

**Table 1.** ERS and $\mathrm{ERS^d}$ *versus* the aspect ratio.

| aspect ratio | ERS ($\mathrm{cm^2}$) | $\mathrm{ERS^d}$ |
|---|---|---|
| 1.5 | 120 | 318 |
| 3.0 | 180 | 241 |
| 5.0 | 380 | 308 |
| 7.1 | 490 | 283 |
| 10.1 | 710 | 287 |

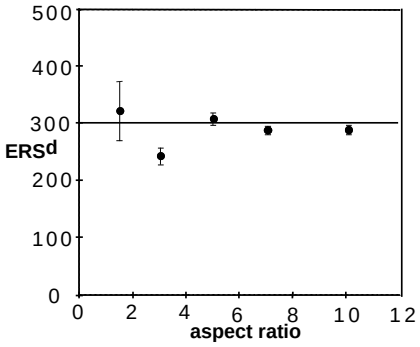


**Fig. 5.** Dimensionless elementary representative surface ($\mathrm{ERS^d}$) *versus* the aspect ratio.

range of aspect ratio, the ERS is equal to $300 \times S_\mathrm{f}$.

$$\mathrm{ERS^d} = \frac{\mathrm{ERS}}{S_\mathrm{f}} \approx 300. \qquad (3)$$

### 2.2.3 Comparison of the two methods

We have compared the two measuring methods through the values of porosity obtained by image processing and by weighing (Tab. 2). It can be seen that there is a good agreement. This seems to show that the cells used are large enough for the boundaries not to have a noticeable effect

**Table 2.** Total areas of the stacks, ERS and porosities.

| aspect ratio | packing area ($cm^2$) | porosity by weighing (%) | ERS ($cm^2$) | porosity by imag. proc. (%) |
|---|---|---|---|---|
| 1.5 | 800 | 27.3 | 120 | 27.05 |
| 3.0 | 810 | 28.6 | 180 | 27.6 |
| 5.0 | 1730 | 31.5 | 380 | 30.3 |
| 7.1 | 1720 | 34.0 | 490 | 33.6 |
| 10.1 | 1700 | 37.2 | 710 | 37.0 |

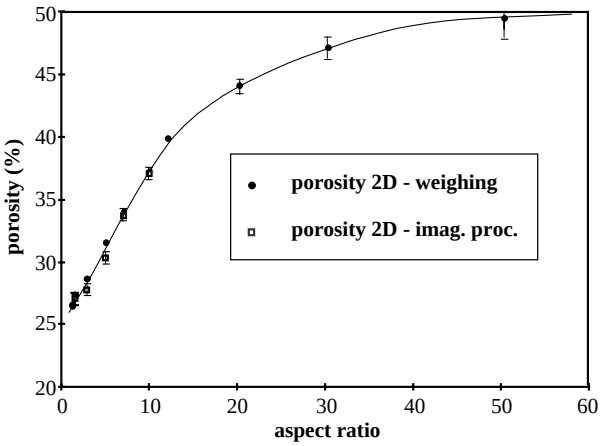


**Fig. 6.** Measured porosity of 2D stacks *versus* the aspect ratio.

**Table 3.** Experimental values of 2D porosities, cells used and number of fibres in the stacks.

| aspect ratio | porosity weighing (%) | porosity imag. proc. (%) | cell | nb of fibres |
|---|---|---|---|---|
| 1.2 | 26.5 | | 1 | 2000 |
| 1.5 | 27.3 | 27.05 | 1 | 2010 |
| 3.0 | 28.6 | 27.6 | 1–2 | 1000 |
| 5.0 | 31.5 | 30.3 | 2 | 1230 |
| 7.1 | 34.0 | 33.6 | 2 | 830 |
| 10.1 | 37.2 | 37.0 | 2 | 550 |
| 12.1 | 39.9 | | 2–3 | 430 |
| 20.2 | 44.1 | | 3 | 540 |
| 30.3 | 47.2 | | 3 | 510 |
| 50.5 | 49.4 | | 3 | 480 |

on the porosity determined by weighing. In these experiments, the total areas of packing are at least 2.4 times larger than the ERS.

## 3 Experimental results

The values of the 2D porosities found by weighing and by image processing are represented in Figure 6. They are given in Table 3 with the numbers of fibres which compose the stacks. All these experimental points correspond to a single curve. 2D porosity is an increasing function of the aspect ratio.

For an aspect ratio equal to 1.2, the porosity of the stack is equal to 26.5%. This stack can be considered as dense. Indeed, for comparison, the lowest porosity for a compact packing of cylinders in 2D would be 21.5%. For high aspect ratios ($r$ close to 50), the porosity is almost 50%.

**Table 4.** Experimental values of 2D and 3D porosities, number of fibres in the stacks.

| aspect ratio | porosity 3D (%) | nb of fibres | porosity 2D (%) | cell | nb of fibres |
|---|---|---|---|---|---|
| 1.2 | 30.9 | 2000 | 26.5 | 1 | 2000 |
| 1.5 | 31.5 | 2010 | 27.3 | 1 | 2010 |
| 3.0 | 33.5 | 1010 | 28.6 | 1 | 1000 |
| 5.0 | 41.7 | 1030 | 31.5 | 2 | 1230 |
| 7.1 | 49.3 | 660 | 34.0 | 2 | 830 |
| 10.1 | 56.2 | 390 | 37.2 | 2 | 550 |
| 12.1 | 63.3 | 280 | 39.9 | 2 | 430 |
| 20.2 | | | 44.1 | 3 | 540 |
| 30.3 | | | 47.2 | 3 | 510 |
| 50.5 | | | 49.4 | 3 | 480 |

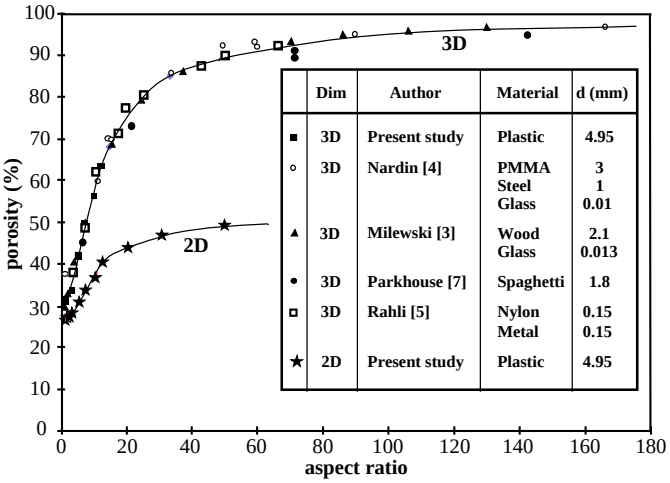


**Fig. 7.** Measured porosities for 2D and 3D stacks *versus* the aspect ratio.

In the absence of a similar system to compare the variation law of the porosity found, we have established a parallel between 2D and 3D packing of fibres (Tab. 4). In Figure 7 the laws of variations are shown for the two types of stacks. We have also mentioned the results of the porosity measurements of 3D stacks found by Milewski [3], Nardin [4], Rahli [5,6] and Parkhouse [8] and we have specified the nature and the characteristics of the fibres used.

It can be noted that for 3D stacks, our experimental plots are very close to the single curve found by the other authors.

The porosity variation laws for 2D and 3D structures are similar. Two behaviours can be observed:

- a noticeably linear variation with a high increase for aspect ratios lower than around 16;
- a zone where the increase is limited with an asymptotic trend for high values of $r$.

It can be seen that the porosity of 2D packing is lower than 3D packing. The deviation between the two curves increases with the aspect ratio.

**Table 5.** Dimensionless excluded volume $V^{\mathrm{f}}_{\mathrm{excl}}$ and number $n$ of fibres in $V^{\mathrm{f}}_{\mathrm{excl}}$ as a function of $r$ for 2D and 3D packing.

| | 3D packing | | | 2D packing | | |
|---|---|---|---|---|---|---|
| aspect ratio | porosity (%) | $V^{\mathrm{f}}_{\mathrm{excl}}$ | $n$ | porosity (%) | $V^{\mathrm{f}}_{\mathrm{excl}}$ | $n$ |
| 1.2 | 30.9 | 9.7 | 6.7 | 26.5 | 5.8 | 4.3 |
| 1.5 | 31.5 | 10.1 | 6.9 | 27.3 | 5.9 | 4.3 |
| 3.0 | 33.5 | 12.6 | 8.4 | 28.6 | 6.9 | 4.9 |
| 5.0 | 41.7 | 16.4 | 9.6 | 31.5 | 8.4 | 5.8 |
| 7.1 | 49.3 | 20.3 | 10.3 | 34.0 | 10.0 | 6.6 |
| 10.1 | 56.2 | 26.3 | 11.5 | 37.2 | 12.4 | 7.8 |
| 12.1 | 63.3 | 30.4 | 11.1 | 39.9 | 14.1 | 8.4 |
| 20.2 | 77 | 46.5 | 10.7 | 44.1 | 20.6 | 11.5 |
| 30.3 | | | | 47.2 | 28.7 | 15.2 |
| 33.3 | 85 | 72.6 | 10.9 | | | |
| 50.0 | 90 | 106.0 | 10.6 | | | |
| 50.5 | | | | 49.4 | 45.1 | 22.8 |

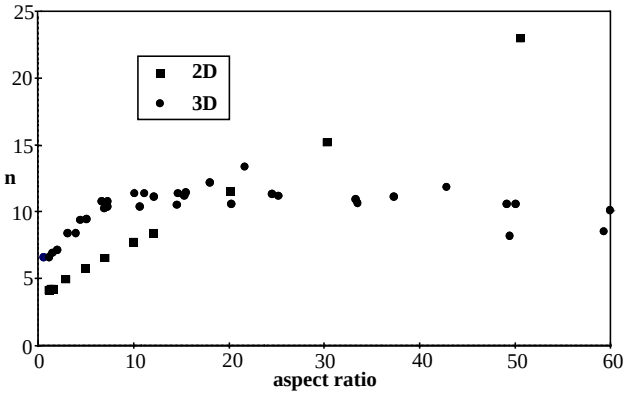


**Fig. 8.** Number $n$ of fibres in the excluded volume for 2D and 3D packing.

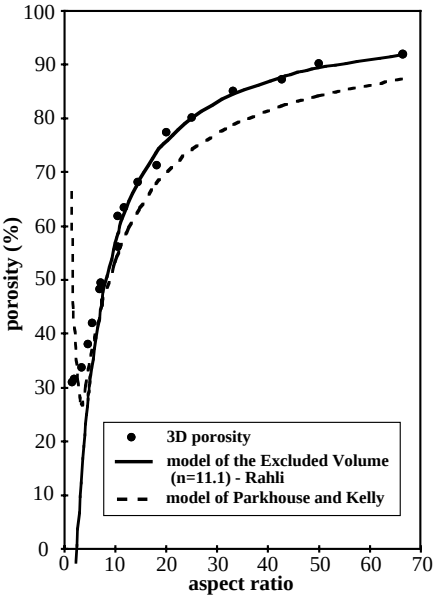


**Fig. 9.** Ranges of validity of the two existing models of variations of the porosity for 3D packing.

## 4 Analysis and interpretation

There exists no theoretical porosity prediction model of a packing of fibres. For 3D stacks, two semi-empirical models have been proposed by Parkhouse and Kelly and by Rahli.

The model of Parkhouse and Kelly [8], based on a statistical approach to the distribution of the pores in the stacks, leads to the following porosity law:

$$\varepsilon \approx 1 - 2\ln(r)/r. \tag{4}$$

Because of the assumptions made in this model, it is limited to 3D packing and cannot be applied to 2D stacks.

Rahli [5,6] proposed a porosity variation law based on the excluded volume model elaborated by Onsager [7]. This volume is defined as the mean portion of the space which one fibre excludes to the centre of the surrounding fibres. By dividing this volume by the volume of a fibre, the dimensionless excluded volume obtained can be written as following:

$$V^{\mathrm{f}}_{\mathrm{excl}} = \frac{\pi}{2r} + 6 + 2r. \tag{5}$$

Rahli proposed the following porosity law:

$$\varepsilon = 1 - \frac{n}{V^{\mathrm{f}}_{\mathrm{excl}}} = 1 - \frac{n}{\dfrac{\pi}{2r} + 6 + 2r} \tag{6}$$

where $n$ is the equivalent number of fibres contained in the excluded volume. For 3D stacks, Rahli [5,6] found that $n$ is noticeably constant and almost equal to 11 for aspect ratios higher than 7 (Tab. 5 and Fig. 8).

The comparison between these two models and the experimental results shows a good qualitative agreement (Fig. 9). Rahli's model gives correct results for aspect ratios higher than 7.

On the basis of these results, we have tried to apply the model of the excluded volume to 2D packing. The detail of the calculation for a fibre having an aspect ratio $r$ is given in the appendix. Thus, the excluded volume obtained for 2D stacks divided by the volume of a fibre can be written as follows:

$$V^{\mathrm{f}}_{\mathrm{excl}} = \frac{8}{\pi} + \frac{16}{\pi^2} + \frac{8}{\pi^2}\left(r + \frac{1}{r}\right). \tag{7}$$

The values calculated from this expression are given in Table 5.

Then, the porosity is:

$$\varepsilon = 1 - \frac{n}{V^{\mathrm{f}}_{\mathrm{excl}}} = 1 - n\left[\frac{8}{\pi} + \frac{16}{\pi^2} + \frac{8}{\pi^2}\left(r + \frac{1}{r}\right)\right]^{-1} \tag{8}$$

where $n$ represents the equivalent number of fibres contained in the excluded volume. It would appear worthwhile to study the behaviour of $n$ for 2D packing. Thus, from the experimental data of porosity we calculate the different values of $n$ (Tab. 5 and Fig. 8).

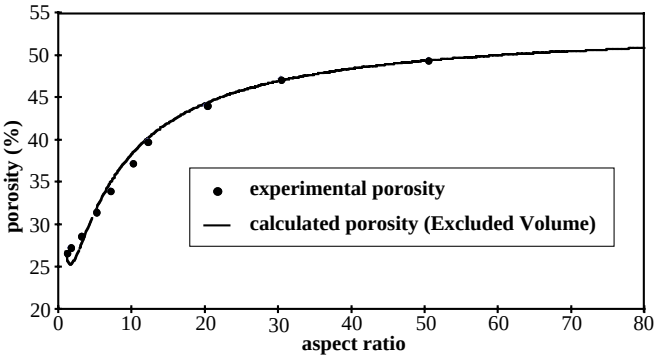


**Fig. 10.** Comparison of the experimental porosities and of the porosities calculated with the excluded volume model for 2D packing.

For the studied aspect ratio range, contrary to 3D packing, the parameter $n$ is noticeably proportional to the aspect ratio.

Using the law found for $n$, the porosity variation according to the aspect ratio can be written as follows:

$$\varepsilon = 1 - \frac{n}{V^{\mathrm{f}}_{\mathrm{excl}}} = 1 - [0.376r + 3.861]\left[\frac{8}{\pi} + \frac{16}{\pi^2} + \frac{8}{\pi^2}\left(r + \frac{1}{r}\right)\right]^{-1}. \quad (9)$$

In Figure 10, a good agreement can be noted between the measured values of the porosity and the values calculated with this equation. For values of $r$ lower than 3, a small deviation appears.

From this equation, we notice a limit of the porosity equal to 53.6% when the aspect ratio of the fibres tends to infinity. According to our experimental results, this limit seems reasonable. If this limit works really for high aspect ratio, it would differ significantly from the limit obtained for 3D packing which is equal to 100%.

However, it is not possible to be sure from experimental data at finite aspect ratio that this difference is maintained in the asymptotic limit of large ratio.

The mechanisms of fibre packing in 3D as well as in 2D cannot be understood from the different models which have been proposed. In Figures 1 (Photos 1 and 2), we observe the existence of dense areas induced by compact stacks and of loose zones due to faulty packing. The compact area is composed of a succession of fibres ordered in the form of bundles while the loose zone is characterised by faulty packing of one or several fibres. Porosity depends on two parameters: the size and the number of the pores. An observation of the stacks does not show up a characteristic pore for a given aspect ratio.

To estimate the influence of the size of the pores on the porosity according to the aspect ratio, a model defect formed by 4 fibres (Fig. 11) was first considered. The elementary cell defined in this way occupies a volume equal to $(L + d)^2 \times d$. The porosity produced by this

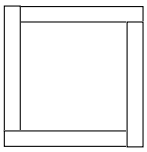

**Fig. 11.** Square elementary cell.

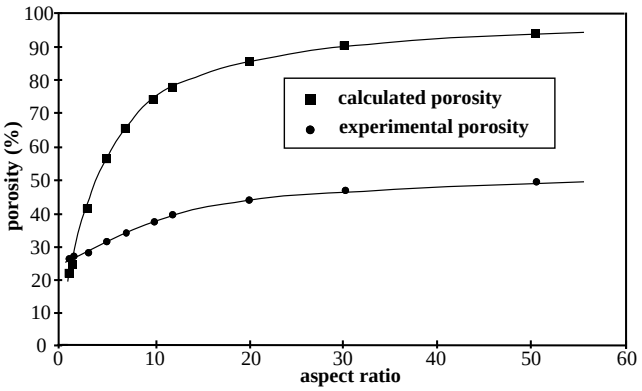


**Fig. 12.** Comparison of the porosities calculated in a square elementary cell and of our experimental porosities.

structure is:

$$\varepsilon = 1 - \pi\frac{r}{(r+1)^2}\cdot \quad (10)$$

In Figure 12, the values of porosity calculated with this expression are compared to our experimental porosities. The curves present an almost similar behaviour. However, the calculated porosities have a sharper increase. In this model, the shapes of the elementary cells and of the pores have been imposed and the number of fibres in a cell has been fixed at 4.

To attempt to generalise this approach, the system is now divided into elementary cells whose shape is not defined precisely and whose volume is $K \times (L+d)^2 \times d$ (where $K$ depends on the geometry of the system). Each of these cells contains a number $n$ of fibres which includes among others the fibres ordered in bundles around the defect. The porosity evaluated in these elementary cells is:

$$\varepsilon = 1 - \pi\frac{n}{K}\frac{r}{(r+1)^2}\cdot \quad (11)$$

The experimental measure of the porosity for an aspect ratio equal to 1.2 gives a value of $n/K$ equal to 0.95. Thus, the porosities calculated with this value are very close to the ones presented in Figure 12 which corresponds to an $n/K$ equal to 1. Figure 13 shows that the values of $n/K$ determined from our experimental porosities increase with the aspect ratio. So, it is essential to increase $n$ and/or to decrease $K$. Indeed, according to Figure 1, it seems obvious that the geometry of the defects and thus the parameter $K$ depend significantly on the aspect ratio of the fibres. So, it is very difficult to describe the system with only one geometry of the pores without taking into account the variation of the shape of the defects with

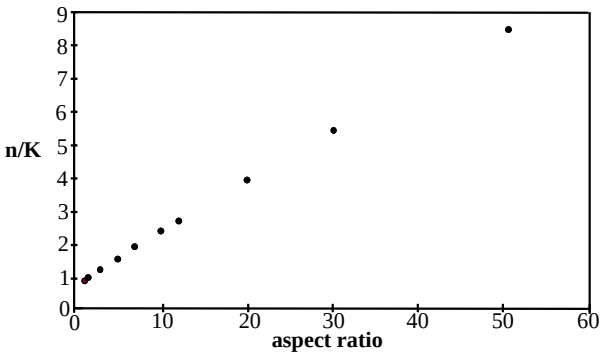


**Fig. 13.** Ratio $n/K$ *versus* the aspect ratio.

the aspect ratio. An approach including the shapes, the sizes and the number of the pores is necessary to uncorrelate the parameters $K$ and $n$ and then to predict the experimental porosity better.

## 5 Conclusion

The Elementary Representative Surface (ERS) for 2D stacks of fibres has been determined. We have shown that the dimensionless ERS does not depend on the aspect ratio.

We have established an experimental law of porosity as a function of the aspect ratio of the fibres for 2D packing.

This variation law is similar to the one corresponding to 3D packing. However, for the same aspect ratio, the 2D stack is more compact.

The excluded volume model for 3D packing has been extended to 2D stacks. We have determined the variation law of the porosity *versus* $r$. The results obtained show that the behaviour of a 3D stack is different from that of a 2D stack. This approach predicts an asymptotic porosity limit equal to 53.6% unlike the 3D case where this limit was equal to 100%. However, this prediction depends on the linearity between $n$ and aspect ratio which, though valid in the experimental range, is not proven in the asymptotic limit of large ratio.

On the basis of the simplified model developed, it seems that the variations of porosity according to the aspect ratio depend on the variation of the size and the shape of the defects.

## Appendix: Calculation of the excluded volume for 2D packing of fibres

The excluded volume has been defined in the previous study as the mean volume which a fibre prevents the centre of its surrounding neighbours from occupying. In 2D, it is convenient to first calculate an excluded surface. Thus, fibres can be considered as rectangles $L$ long and $d$ large.

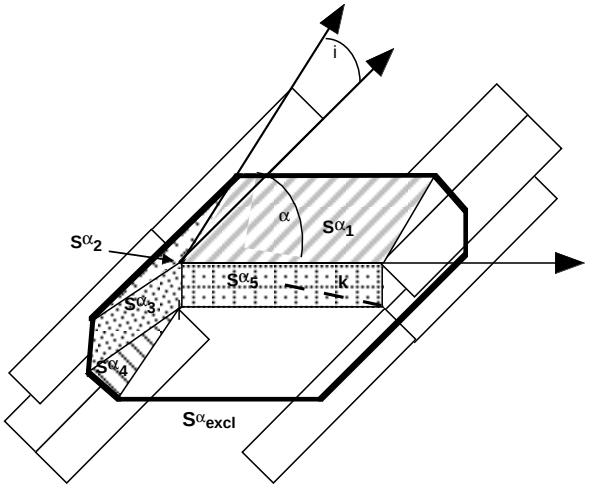


**Fig. 14.** Representation of the excluded volume in 2D for 2 fibres making an angle $\alpha$.

First of all, it is necessary to calculate the excluded surface $S^{\alpha}_{\text{excl}}$ for two fibres making an angle $\alpha$. In practice, to calculate $S^{\alpha}_{\text{excl}}$, we make one fibre slide along the other one while maintaining their orientation as shown in Figure 14.

So, the excluded surface $S^{\alpha}_{\text{excl}}$ can be broken down as following:

$$S^{\alpha}_{\text{excl}} = 2(S^{\alpha}_1 + S^{\alpha}_2 + S^{\alpha}_3 + S^{\alpha}_4) + S^{\alpha}_5.$$

Let $k$ be the half of the diagonal of a rectangle, the calculation of the different surfaces leads to the following expressions:

$$\begin{aligned} S^{\alpha}_1 &= L \times k \times \sin(\alpha + i) \\ S^{\alpha}_2 &= S^{\alpha}_4 = \frac{Ld}{4} \\ S^{\alpha}_3 &= d \times k \times \cos(\alpha - i) \\ S^{\alpha}_5 &= L \times d. \end{aligned}$$

So, we obtain the following expression for the excluded surface for 2 fibres making an angle $\alpha$:

$$S^{\alpha}_{\text{excl}} = 2Ld + 2Lk\sin(\alpha + i) + 2dk\cos(\alpha - i).$$

Then, it is possible to calculate the excluded surface by averaging the previous expression over all the possible relative orientations $\alpha$ between the 2 fibres:

$$S_{\text{excl}} = \frac{1}{\pi/2}\int_0^{\pi/2} [2Ld + 2Lk\sin(\alpha + i) + 2dk\cos(\alpha - i)]\mathrm{d}\alpha$$

which can be written:

$$S_{\text{excl}} = 2Ld + \frac{4}{\pi}k[\sin(i) + \cos(i)][L + d].$$

Now, with the following relations:

$$k = \sqrt{\left(\frac{L}{2}\right)^2 + \left(\frac{d}{2}\right)^2}, \quad \sin(i) = \frac{d}{\sqrt{(L^2 + d^2)}} = \frac{d}{2k}$$

and

$$\cos(i) = \frac{L}{\sqrt{(L^2 + d^2)}} = \frac{L}{2k}$$

we find:

$$S_{\text{excl}} = 2Ld + \frac{2}{\pi}[L + d]^2.$$

To obtain the excluded volume $V_{\text{excl}}$, we have to multiply the previous expression by the diameter $d$ of a fibre. Then, by dividing the resulting relation by the volume of a fibre, we obtain the dimensionless excluded volume:

$$V_{\text{excl}}^{\text{f}} = \frac{8}{\pi} + \frac{16}{\pi^2} + \frac{8}{\pi^2}\left(r + \frac{1}{r}\right).$$

## References


1. J.V. Milewski, in *28th Annual Technical Conference, Reinforced Plastics/Composites Institute, The Society of the Plastics Industry, Inc. (1973).*
2. J.V. Milewski, Ind. Eng. Chem. Prod. Res. Dev. **17**, 363 (1978).
3. J.V. Milewski, Adv. Ceramic Mater. **1**, 36 (1986).
4. M. Nardin, E. Papirer, J. Schultz, Powder Technol. **44**, 131 (1984).
5. O. Rahli, Ph.D. thesis, University of Provence, 1997.
6. O. Rahli, L. Tadrist, R. Blanc, C. R. Acad. Sci. Paris **327**, serie IIb (1999).
7. L. Onsager, Ann. New York (Academy of Sciences) 627 (1948).
8. J.G. Parkhouse, A. Kelly, Proc. R. Soc. Lond. A **451**, 737 (1995).